Macromolecular Research, Vol. 14, No. 2, pp 166-172 (2006)

The Allosteric Transition of the Chaperonin GroEL from *Escherichia coli* as Studied by Solution X-Ray Scattering

Kunihiro Kuwajima*, Tomonao Inobe, and Munehito Arai

Department of Physics, Graduate School of Science, University of Tokyo, 7-3-1 Hongo, Bunkyo-ku, Tokyo 113-0033, Japan

Received September 22, 2005; Revised January 18, 2006

Abstract: This is a short review article of our recent studies on the ATP-induced, allosteric conformational transition of the chaperonin GroEL complex by solution X-ray scattering. We used synchrotron X-ray scattering with a two-dimensional, charge-coupled, device-based X-ray detector to study (1) the specificity of the chaperonin GroEL for its ligand that induced the allosteric transition, and (2) the identification of the allosteric transition of GroEL in its complicated kinetics induced by ATP. Due to the dramatically increased sensitivity of the X-ray scattering technique based on the use of the two dimensional X-ray detector and synchrotron radiation, different allosteric conformational states of GroEL populated under different conditions were clearly distinguished from each other. It was concluded that solution X-ray scattering is an extremely powerful tool for investigating the equilibrium and kinetics of cooperative conformational transitions of oligomeric protein complex, especially when combined with other spectroscopic techniques such as fluorescence spectroscopy.

Keywords: allosteric transition, chaperonin GroEL, X-ray scattering.

Introduction

Chaperonins are a class of molecular chaperones that promote protein folding in a biological cell and are widely found in biological organisms, including bacteria, chloroplasts, mitochondria, archaea, and eukaryotic cytosol.[1,2] The chaperonin GroEL from *Escherichia coli* is best characterized among the chaperonins. It is a tetradecameric protein complex of 14 identical 57 kDa subunits arranged in two heptameric rings stacked back-to-back with a central cavity (Figure 1).[2] A single subunit of GroEL is composed of three domains: (1) an apical domain that forms an opening of the ring and exposes a number of hydrophobic amino-acid residues toward the center of the GroEL ring, (2) an equatorial domain that contains the nucleotide-binding site and makes the foundation of the GroEL ring structure, and (3) an intermediate domain that joins the apical and equatorial domains.

SAXS is very effective as a technique to investigate overall shape and dimension of a protein and a protein complex in solution.[3] We used synchrotron SAXS to study GroEL, and employed a two-dimensional (2D) charge-coupled device (CCD)-based X-ray detector with a beryllium-windowed X-ray image intensifier.[4-6] The experiments were carried out at the beam line 15A of the photon factory at the High Energy Research Organization, Tsukuba, Japan. Figure 2 compares raw scattering data of the chaperonin GroEL solution measured by the 2D CCD-based X-ray detector and by a one-dimensional position sensitive proportional counter (1D PSPC).[5] We can see dramatic improvement of the signal-to-noise ratio of the data obtained by the 2D CCD-based detector, and this allowed us to carry out kinetic measurements with a time resolution of 10 ms by combination with a stopped-flow apparatus.

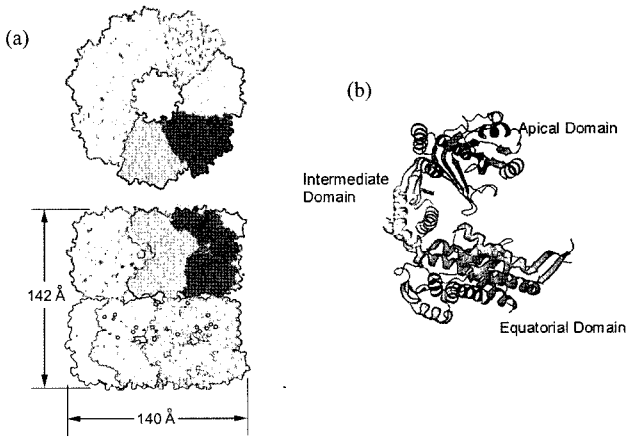

Figure 1. The structure of the *E. coli* chaperonin GroEL (PDB code: 1OEL). (a) A space-filling model of the GroEL particle (the top view (upper) and the side view (lower)). (b) A ribbon model of a subunit of GroEL.

*Corresponding Author. E-mail: kuwajima@phys.s.u-tokyo.ac.jp

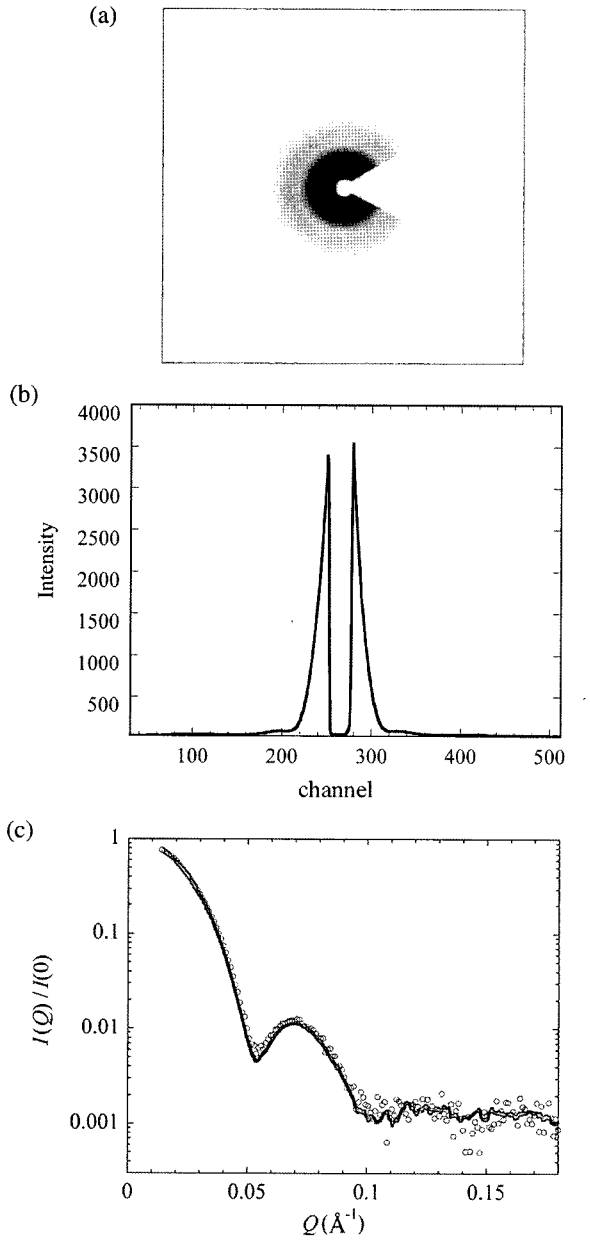

Figure 2. (a) Raw scattering data of the chaperonin GroEL solution measured by the 2D CCD-based X-ray detector and (b) by the 1D PSPC. (c) The X-ray scattering curves of chaperonin GroEL under the native conditions measured by the CCD-based X-ray detector (thick lines) and by the PSPC (open circles). Protein concentration was 10 mg/mL. The channel width of the CCD data was 0.1535 mm, while that of the PSPC data was 0.368 mm. Total exposure time to X-ray beam was 170 and 800 s for the measurement by the CCD-based X-ray detector and the PSPC, respectively. The figure was from ref. (5) with permission.

GroEL is known to undergo cooperative allosteric transition induced by ATP, and the allosteric transition must be important for functional activities of the chaperonin as a molecular chaperone.[7,8] We have recently studied the allosteric transition of GroEL induced by ATP and also by a series of metal fluoride-ADP complexes using small angle X-ray scattering (SAXS) and fluorescence spectroscopy in combination with a stopped-flow technique, and this paper is a summary review of these studies.

The Allosteric Transition of GroEL

There are two levels of the allosteric transition of GroEL induced by ATP, one within each ring and the second between the rings. In the first level, the allosteric transition occurs from the T to the R state in accordance with the Monod-Wyman-Changeux (MWC) model, with positive cooperativity with respect to ATP, where T and R denote tense and relaxed states, respectively, for a single-ring part of the GroEL complex.[7] In the second level of allostery, GroEL undergoes sequential Koshland-Némethy-Filmer (KNF)-type transitions from the TT via the TR to the RR state with negative cooperativity between the rings. The ATP-dependent control of the affinity of GroEL for its target protein and resulting facilitation of protein folding are underpinned by the allosteric transition.

Because GroEL has a weak ATPase activity, its allosteric transition can be observed by monitoring the ATPase activity as a function of ATP concentration. Figure 3 shows the allosteric transition as measured by the initial rate (V_i) of ATP hydrolysis by GroEL.[9] The first level of the transition between TT and TR is observed below 100 μM and characterized by a sigmoidal dependence of V_i on ATP concentration, and the second level of the transition occurs above 100 μM, where V_i decreases with ATP concentration.

Currently, important issues on the ATP-induced allosteric transition of GroEL may include : (1) Why GroEL has strikingly high specificity for ATP as an effective allosteric ligand,[10] and (2) identification of the allosteric conformational transition in complex kinetics of GroEL observed by fluorescence and other spectroscopic techniques.[11] The allosteric transition of GroEL has so far only been investigated by the ATPase assay or fluorescence spectroscopy of tryptophan mutants or a pyrene-labeled form of GroEL,[9,12,13] and hence direct structural data by SAXS should give us further insight into these issues.

Synchrotron SAXS Can Distinguish between Different Allosteric States of GroEL

SAXS can clearly distinguish the three allosteric states, TT, TR, and RR. Figure 4 shows the SAXS profiles of GroEL in the three states. The scattering pattern in the TT state in the absence of ATP exhibits characteristic double maxima at Q values of 0.12 and 0.17 Å^{-1}, where Q is given by $Q=(4\pi\sin\theta)/\lambda$, and 2θ and λ are scattering angle and wavelength (1.5 Å), respectively. In the scattering pattern in the TR state at 85 μM ATP, the double maxima collapse into

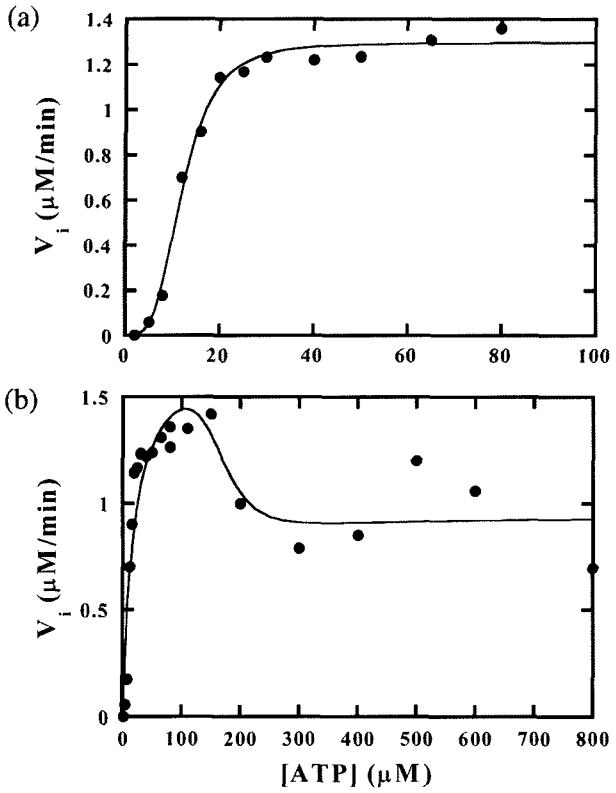

Figure 3. Initial velocities of ATP hydrolysis by GroEL (a) at lower ATP concentrations up to 100 μM, and (b) at higher ATP concentrations above 100 μM. The reactions were carried out in 50 mM Tris-HCl (pH 7.5), 10 mM KCl, and 10 mM $MgCl_2$ at 23 °C. The monomeric concentration of protein was 420 nM. The Figure was from ref. (9) with permission.

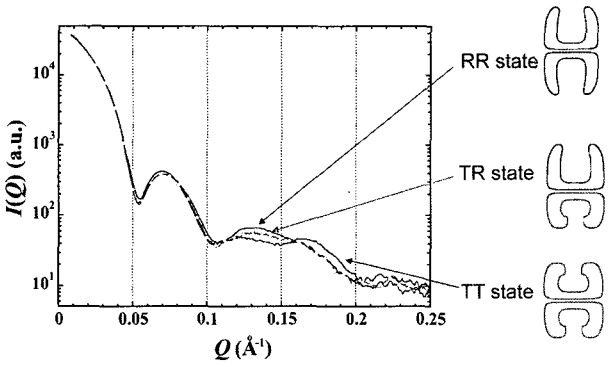

Figure 4. SAXS patterns of GroEL at 0 M (black solid line), 85 μM (solid line with open circles), and 3 mM ATP (gray solid line) at 25 °C. The scattering intensity $I(Q)$ is shown as a function of Q. The scattering curves were measured at concentrations between 3-7 mg/mL. The scattering data below 0.025 Å^{-1} were extrapolated to zero concentration. At high angle region (Q > 0.025 Å^{-1}), the data only for one concentration are shown (7 mg/mL and 3 mg/mL GroEL for TT/RR state and TR state, respectively). The Figure was from ref. (11) with permission.

a single maximum at 0.13 Å^{-1}, and the intensity between 0.06 and 0.08 Å^{-1} decreases significantly, both of which may reflect the TT to TR allosteric conformational transition of GroEL. A preliminary analysis of the scattering patterns by a program of CRYSOL[14] has suggested that the changes in the scattering pattern during the TT to TR transition are consistent with cooperative twisting up of the apical domains in the *cis* ring as suggested by electronmicroscopy studies[15]; the *cis* ring is the ring to which seven ATP molecules are bound. At 3 mM ATP, where GroEL is in the RR state, the scattering pattern shows further changes, and the intensity between 0.11 and 0.16 Å^{-1} increases.

Specificity of GroEL for Its Ligand that Induces the Allosteric Transition

Figure 5 shows fluorescence titration curves of pyrene-labeled form of GroEL titrated with ADP, ATP analogs (AMP-PNP, and ATPγS), and ATP, in which the observed fluorescence change at 375 nm, ΔF_{obs}, is plotted as a function of the ligand concentration, [S].[9] Only ATP induces the cooperative allosteric transition as shown by a sigmoidal titration curve (Figure 5(c)), which is phenomenologically well fitted to the following equation with a Hill coefficient, n_H, of 2.5:

$$\Delta F_{obs} = \Delta F \frac{K_{app}[S]^{n_H}}{1 + K_{app}[S]^{n_H}} \quad (1)$$

where K_{app} is the apparent binding constant of ATP to GroEL. On the other hand, the titration curves with ADP, AMP-PNP and ATPγS are consistent with non-cooperative bindings to two independent binding sites, and well fitted to the equation:

$$\Delta F_{obs} = \Delta F_1 \frac{K_{b1}[S]}{1 + K_{b1}[S]} + \Delta F_2 \frac{K_{b2}[S]}{1 + K_{b2}[S]} \quad (2)$$

where ΔF_1 and ΔF_2 are total fluorescence changes, and similarly K_{b1} and K_{b2} are binding constants for the first and second sites, respectively. The difference between ATP and the ATP analogs is rather surprising, because for example, there is an only very subtle difference in the γ-phosphate group between ATP and ATPγS.

To further investigate the specificity of GroEL for its ligand, we studied the effect of a series of metal-fluoride ADP complexes and vanadate-ADP on GroEL by small-angle X-ray scattering.[10] The metal fluorides and vanadate, complexed with ADP, are known to mimic the γ-phosphate group of ATP (Figure 6), but they differ in geometry and size; it is expected that these compounds will be useful for investigating the strikingly high specificity of GroEL for ATP that enables the induction of the allosteric transition.

Figure 7 shows X-ray scattering patterns of GroEL in the

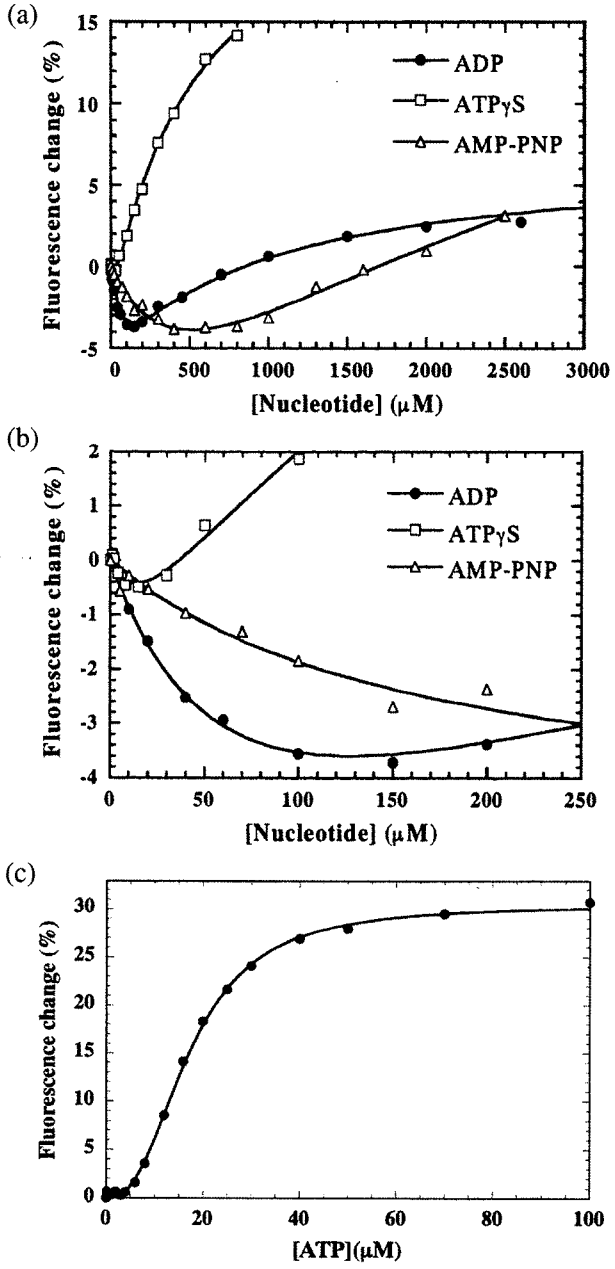

Figure 5. (a) and (b) The fluorescence change of pyrenyl-GroEL at different nucleotide concentrations, and (c) the fluorescence-detected ATP titration of pyrenyl-GroEL. (a) and (b) Pyrenyl-GroEL and nucleotide were mixed at 25 °C, yielding the final concentration of 700 nM monomeric subunit and a given concentration of nucleotide, and the fluorescence change at 375 nm was recorded. Symbols indicate as follows: ADP (●); ATPγS (□); and AMP-PNP (△). The solid line shows the optimal fit of the data to two saturation curves, indicating noncooperative binding. The data for the nucleotide titration to pyrenyl-GroEL at nucleotide concentration below 200 μM are shown in panel (b). (c) One volume of ATP solution was added to 4 volumes of 62.5 nM pyrenyl-GroEL for a final concentration of 50 nM, and the fluorescence change at 375 nm was recorded. The figure was from ref. (9) with permission.

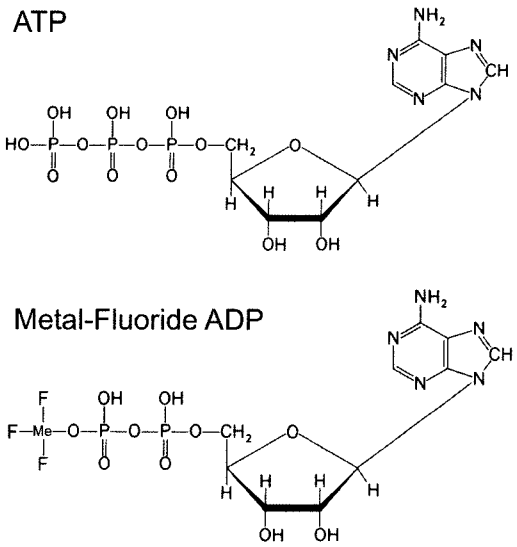

Figure 6. Chemical structures of ATP and metal-fluoride ADP complex.

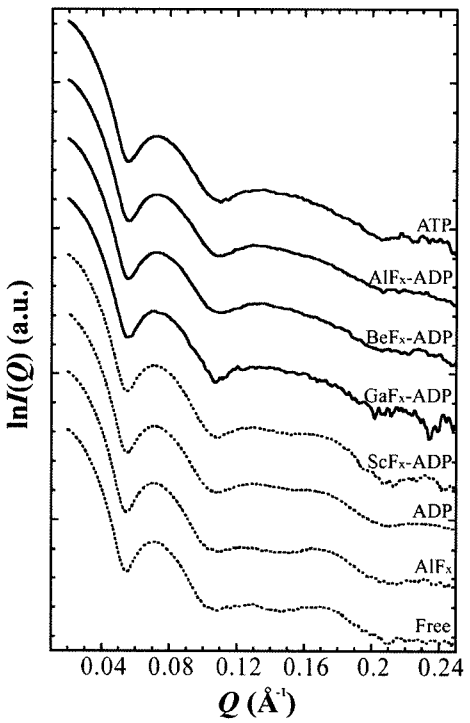

Figure 7. The X-ray scattering patterns of GroEL in the various nucleotide/γ-phosphate analog conditions. The scattering intensity $I(Q)$ is shown as a function of Q. From the top: in the presence of ATP, AlF_x plus ADP, BeF_x plus ADP, GaF_x plus ADP, ScF_x plus ADP, ADP alone, and AlF_x alone, and in the absence of both the nucleotide and the γ-phosphate analog. The scattering data at 7 mg/mL GroEL are shown. Each line has been shifted such that it can be clearly seen. The scattering patterns shown by solid lines indicate the occurrence of the allosteric transition, while those shown by broken lines indicate the absence of the transition. The figure was from ref. (10) with permission.

Table I. The Presence or Absence of the Allosteric Transition of GroEL by Various ADP-γPhosphate Analogs, and Coordination Number, Geometry, and Size of the Phosphate Analogs[a]

Phosphate Analog	Allosteric Transition	Coordination No. and Geometry of Metal	Inter-atomic Distance	Ion Radius
AlF_x	Yes	4 (?)	1.63	0.53
BeF_x	Yes	4 (Td)[b]	1.53	0.41
GaF_x	Yes	4 (Td)	-	0.61
P_i	No	4	1.6	0.31
ScF_x	No	6 (Oh)	2.06-2.18	0.88
V_i	No	5 (tbp)	2.24	0.5

[a]The table was from ref. (10) with permission.
[b]Td = tetrahedral, Oh = octahedral, and tbp = trigonal bipyramidal.

various nucleotide/γ-phosphate analog conditions.[10] The results indicate that the allosteric state induced by these metal fluoride-ADP complexes is structurally equivalent to the allosteric state induced by ATP, and that both the size and coordination geometry of γ-phosphate (and its analogs) are related to the allosteric transition of GroEL. Table I summarizes coordination number, geometry, and size of various phosphate analogs used in this study.[10] It is thus concluded that the tetrahedral geometry of γ-phosphate (or its analogs) and the inter-atomic distance (~1.6 Å) between phosphorous (vanadium, or metal atom) and oxygen (or fluorine) are both important for inducing the allosteric transition of GroEL, leading to the high selectivity of GroEL for ATP about ligand adenine nucleotides, which function as the preferred allosteric ligand. Confinement of the γ-phosphate of ATP to a small space available in the nucleotide binding site may result in tight binding of ATP to GroEL, increasing the binding affinity of the ligand, but may remarkably enhance the specificity for the ligand as well.[10]

Kinetics of the Allosteric Transition of GroEL Monitored by Stopped-Flow SAXS and Fluorescence

The kinetics of the allosteric transition of GroEL induced by ATP were previously studied by a stopped-flow fluorescence technique by monitoring tryptophan fluorescence of tryptophan mutants of GroEL.[12,13] The kinetics were complicated with at least four exponential phases, and hence there was the question which of the four phases corresponded to the allosteric transition of GroEL.

We thus used the stopped-flow X-ray scattering to investigate the kinetics of the transition of GroEL induced by 85 μM ATP at 4.8 °C.[11] The resultant kinetic progress curve shown in Figure 8(a) is a time course of the integral intensity of the X-ray scattering in a region of Q between 0.06 and 0.08 $Å^{-1}$. The intensity is first decreased with a rate constant of 3.4 s^{-1}, followed by a small linear increase in the intensity. The first

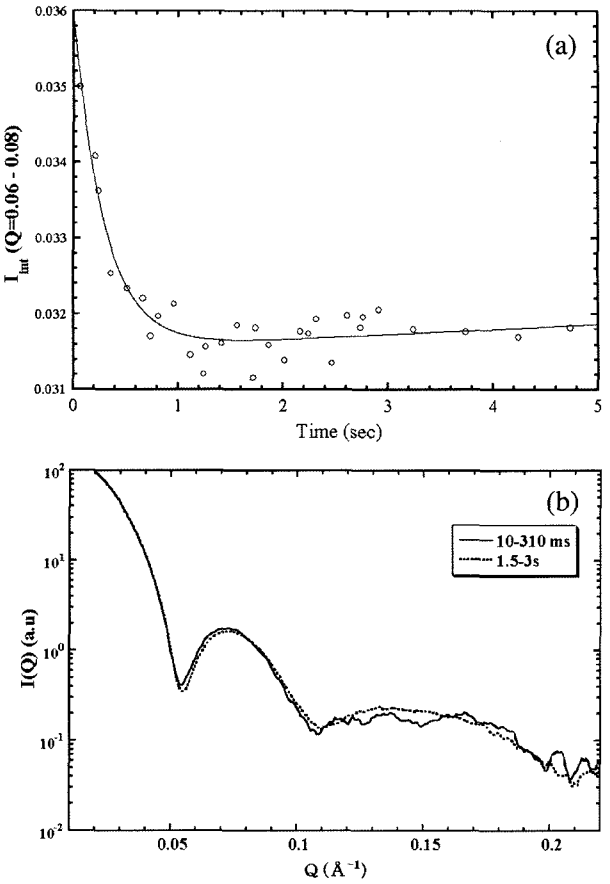

Figure 8. (a) A kinetic curve of the ATP-induced structural change of GroEL at 4.8°C monitored by the integral intensity I_{int} of X-ray scattering. The integral region of Q employed was from 0.06 to 0.08 $Å^{-1}$. The structural change was initiated by a mixing with ATP (final concentrations of 3.8 μM (3 mg/mL) and 85 μM for GroEL and ATP, respectively). The solid line shows a theoretical kinetic progress curve assuming a single exponential with the equation: $I_{int}(t)=Ae^{-kt}+Bt+C$, where A and k are the amplitude and the rate constant of the exponential phase, B and C are constants. The second term Bt is introduced for the purpose of correcting linear increase in the scattering intensity caused by beam damage (see text). (b) The SAXS patterns were averaged between 10 and 310 ms (solid line) and between 1.5 and 3 sec (broken line). The figure was from ref. (11) with permission.

decrease in the intensity reflects the allosteric (TT to TR) transition of GroEL, and the small linear increase in the intensity may be caused by beam damage of the protein by X-ray. Figure 8(b) shows transient scattering patterns of GroEL averaged between 10 and 310 ms and between 1.5 and 3 s after induction of the allosteric transition by ATP.[11] The two scattering patterns are coincident with the static scattering patterns in the TT and TR states (Figure 3), respectively, indicating that the above first decrease in the kinetics measured by the integral intensity results from the TT to TR transition, and this kinetics has been found to be

identical with the second phase of the kinetics measured by fluorescence.

Because the second phase of the multiphasic kinetics measured by tryptophan fluorescence was identified as the allosteric transition, we next studied the second phase more in detail by the use of a tryptophan mutant (Y485W) of GroEL.[11] Figure 9 shows the rate constant and the amplitude change of the second phase measured by stopped-flow fluorescence as a function of ATP concentration. Both the observed rate constant (k_{obs}) and amplitude change (α_{obs}) show sigmoidal dependence on ATP concentration, reflecting the cooperativity of the allosteric transition. The dependence of k_{obs} and α_{obs} on ATP concentration is well represented by a

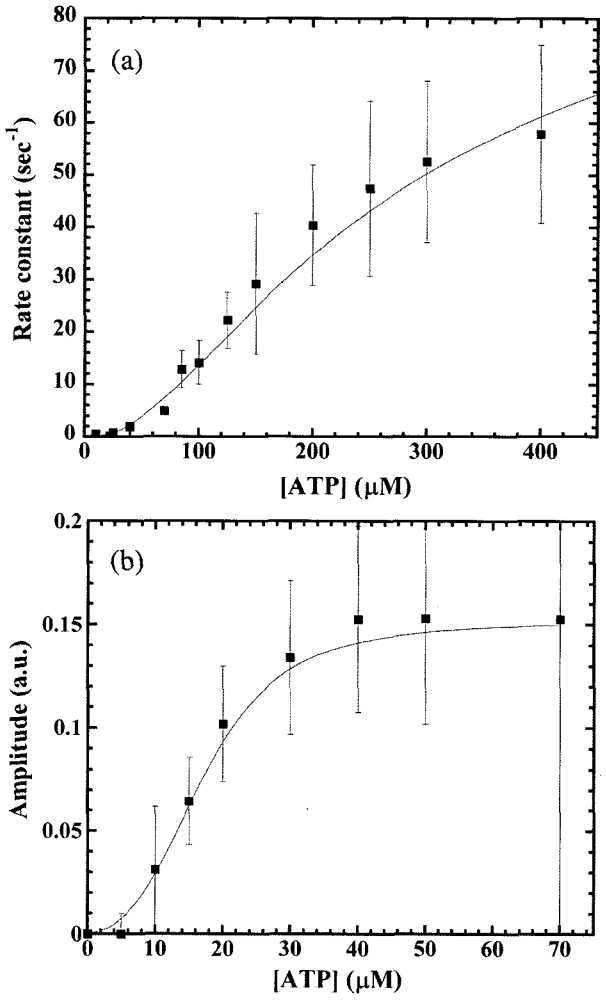

Figure 9. Kinetic parameters of the fluorescence change of Y485W when it is mixed with ATP at 25.4 °C. (a) The observed rate constant and (b) the amplitude at the second phase of the ATP-induced fluorescence change as a function of ATP concentration. The data of the rate constant and the amplitude at the second phase were simultaneously fitted to equations (3) and (4), respectively (solid lines). The buffer used in this measurement was 50 mM Tris-HCl (pH 7.5), 10 mM $MgCl_2$, and 10 mM KCl. The figure was from ref. (11) with permission.

combination of the conventional MWC allosteric model and the transition state theory, in which the T state (TT state) that is stable in the absence of ATP is cooperatively transformed into the R state (TR state) through a single transition state (‡ state) that is the state of maximum free energy between the T and R states.[11,16] The cooperative transconformation is linked with ATP binding, because there are multiple (seven) binding sites in one ring of GroEL with the binding constant in the R state (K_b^R) being larger than that in the T state (K_b^T). The dependence of k_{obs} and α_{obs} on ATP concentration ([S]) is thus given by the equations:

$$k_{obs}^{2nd} = k_{TR}^0 \frac{(1+K_b^{\ddagger}[S])}{(1+K_b^T[S])^7} + k_{RT}^0 \frac{(1+K_b^{\ddagger}[S])}{(1+K_b^R[S])^7} \quad (3)$$

$$\alpha^{2nd} = \frac{L(1+K_b^R[S])^7}{(1+K_b^T[S])^7 + L(1+K_b^R[S])^7} \quad (4)$$

where $K_b^{\ddagger}$ is the binding constant in the ‡ state, k_{TR}^0 and k_{RT}^0 are the microscopic rate constants of the T to R and the R to T transitions in the absence of ATP, respectively, and L equal to k_{TR}^0/k_{RT}^0. The parameters obtained by simultaneous nonlinear least squares fitting of the data of Figure 9 to eqs. (3) and (4) are $K_b^T = 22(\pm 4)\times 10^3$ M^{-1}, $K_b^R = 140(\pm 10)\times 10^3$ M^{-1}, $K_b^{\ddagger} = 130(\pm 90)\times 10^3$ M^{-1}, $k_{RT}^0 = 0.15(\pm 0.55)$ s^{-1}, and $k_{TR}^0 = 3(\pm 11)\times 10^{-4}$ s^{-1}. Because $K_b^{\ddagger}$ is similar to K_b^R, the transition state of the allosteric conformational change of GroEL is more similar to the R state than to the T state.

Figure 10 shows a schematic representation of the GroEL allosteric transition induced by ATP. This simple two-state model can well interpret the rate constant and the amplitude change of the allosteric transition kinetics measured by stopped-flow fluorescence.

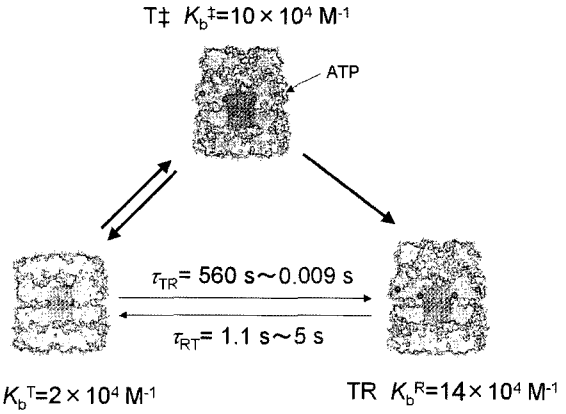

Figure 10. A schematic representation of the GroEL allosteric transition induced by ATP. The relaxation times, τ_{TR} and τ_{RT}, are the reciprocals of the microscopic rate constants, k_{TR} and k_{RT}, respectively, and change with ATP concentration. Following equation (3), k_{TR} and k_{RT} are given by $k_{TR}=k_{TR}^0(1+K_b^{\ddagger}[S])/(1+K_b^T[S])^7$ and $k_{RT}=k_{RT}^0(1+K_b^{\ddagger}[S])/(1+K_b^R[S])^7$, respectively.

Conclusions

Both of the above studies thus clearly indicate that the solution X-ray scattering is extremely powerful for investigating the equilibrium and kinetics of cooperative conformational transitions of oligomeric protein complexes, especially when combined with other spectroscopic techniques such as fluorescence spectro-scopy. Major conclusions obtained in the above studies are:

(1) By the use of synchrotron X-ray scattering, we observed high selectivity for the allosteric ligand complex in a series of the metal fluoride ADP and vanadate-ADP complexes. This selectivity is probably due to confinement of the γ-phosphate of ATP to a small space available in the nucleotide-binding site of GroEL leading to the high selectivity of GroEL for ATP as the ligand.

(2) The stopped-flow X-ray scattering study has shown that the transition from the close (TT) to the open (TR) state of GroEL occurs after binding by ATP with an apparent rate constant of 3.4 s at 4.8 °C and 85 μM ATP. This process corresponds to the second phase of the multi-phase kinetics of GroEL (Y458W) observed by stopped-fluorescence.

Another unresolved question of the chaperonin complex at present is concerning "What kind of structure does the GroEL/ES complex form in a biological cell?" There are two possibilities on this issue: (1) A one (GroEL) to one (GroES) bullet-type complex, and (2) a one (GroEL) to two (GroES) football-type complex. Although many studies have suggested the bullet-type complex is the major species, electron-microscopic studies have demonstrated the existence and importance of the football-type complex,[17-19] and this question has been controversial.[20] The solution X-ray scattering should be very effective to distinguish between these two types of the complexes, and in fact, our preliminary studies by X-ray scattering have shown that only the bullet type complex is detected under naturally occurring native conditions.

Acknowledgements. We thank Professors Y. Amemiya, H. Kihara, and K. Wakabayashi, and Drs. K. Ito, K. Kamagata, K. Maki, and M. Nakao for their assistance and useful discussions. This study was supported by Grants-in-Aid for Scientific Research from the Ministry of Education, Culture, Sports, Science and Technology of Japan, and performed under approval of the Photon Factory (Proposal No. 2000G325).

References

(1) H. R. Saibil, A. L. Horwich, and W. A. Fenton., *Adv. Protein Chem.*, **59**, 45 (2001).
(2) P. B. Sigler, Z. H. Xu, H. S. Rye, S. G. Burston, W. A. Fenton, and A. L. Horwich, *Annu. Rev. Biochem.*, **67**, 581 (1998).
(3) O. Glatter and O. Kratky, *Small angle X-ray scattering*, Academic Press, London, 1982.
(4) K. Ito and Y. Amemiya, *J. Jpn. Soc. Synchrotron Rad. Res.*, **13**, 372 (2000).
(5) M. Arai, K. Ito, T. Inobe, M. Nakao, K. Maki, K. Kamagata, H. Kihara, Y. Amemiya, and K. Kuwajima, *J. Mol. Biol.*, **321**, 121 (2002).
(6) K. Kuwajima, M. Arai, T. Inobe, K. Ito, M. Nakao, K. Maki, K. Kamagata, H. Kihara, and Y. Amemiya, *Spectroscopy-Int. J.*, **16**, 127 (2002).
(7) O. Yifrach and A. Horovitz, *Biochemistry*, **34**, 5303 (1995).
(8) A. Horovitz, *Current Opinion in Structural Biology*, **8**, 93 (1998).
(9) T. Inobe, T. Makio, E. Takasu-Ishikawa, T. P. Terada, and K. Kuwajima, *Biochim. Biophys. Acta*, **1545**, 160 (2001).
(10) T. Inobe, K. Kikushima, T. Makio, M. Arai, and K. Kuwajima, *J. Mol. Biol.*, **329**, 121 (2003).
(11) T. Inobe, M. Arai, M. Nakao, K. Ito, K. Kamagata, T. Makio, Y. Amemiya, H. Kihara, and K. Kuwajima, *J. Mol. Biol.*, **327**, 183 (2003).
(12) O. Yifrach and A. Horovitz, *Biochemistry*, **37**, 7083 (1998).
(13) M. J. Cliff, N. M. Kad, N. Hay, P. A. Lund, M. R. Webb, S. G. Burston, and A. R. Clarke, *J. Mol. Biol.*, **293**, 667 (1999).
(14) D. Svergun, C. Barberato, and M. H. J. Koch, *J. Appl. Crystallogr.*, **28**, 768 (1995).
(15) A. M. Roseman, S. X. Chen, H. White, K. Braig, and H. R. Saibil, *Cell*, **87**, 241 (1996).
(16) T. Inobe and K. Kuwajima, *J. Mol. Biol.*, **339**, 199 (2004).
(17) A. Azem, M. Kessel, and P. Goloubinoff, *Science*, **265**, 653 (1994).
(18) O. Llorca, S. Marco, J. L. Carrascosa, and J. M. Valpuesta, *FEBS Lett.*, **345**, 181 (1994).
(19) M. Schmidt, K. Rutkat, R. Rachel, G. Pfeifer, R. Jaenicke, P. Viitanen, G. Lorimer, and J. Buchner, *Science*, **265**, 656 (1994).
(20) F. J. Corrales and A. R. Fersht, *Folding and Design*, **1**, 265 (1996).